Geotechnical Engineering in the XXI Century: Lessons learned and future challenges
N.P. López-Acosta et al. (Eds.)

doi:10.3233/STAL190044

Shearing of Clay-Structure Interfaces at Varying Deformation Rates

Alejandro MARTINEZ[a,1] and Hans Henning STUTZ[b]
[a] *Department of Civil and Environmental Engineering, University of California Davis, USA*
[b] *Department of Engineering, Aarhus Universitet, Denmark*

Abstract. Many types of geotechnical systems rely on the transfer of load across soil-structure interfaces, including deep foundations, earth retaining structures, landfills, and seabed pipelines. The loading applied to these interfaces can induce soil deformations at widely different strain rates which can control their strength. This paper describes the results from a laboratory study on the interface shear behavior of clay-structure interfaces at varying deformation/shear rates. The results of shear box tests on kaolinite specimens sheared against surfaces of varying roughness indicate that as the shear rate is increased the drainage conditions at the interface change from drained to partially drained to undrained. This change in drainage conditions, from drained to undrained, results in a decrease in shear strength on normally-consolidated clay specimens due to generation of excess pore pressures. On the other hand, shearing at faster rates results in an increase in shear strength in over-consolidated specimens due to generation of negative pore pressures. Particle Image Velocimetry (PIV) analyses indicate that soil deformations at the meso-scale decrease as the shearing rate is increased. The results presented herein highlight the role of surface roughness on the mobilization of interface strength, and provides new evidence that surface roughness can alter the drainage conditions mobilized at the interface.

Keywords. Soil-structure interaction, interface shearing, laboratory testing, clay.

1. Introduction

The strength and deformation behavior of soil-structure interfaces is of great importance for the capacity and safety of many geotechnical structures, such as deep foundations, earth retaining structures, landfills, seabed pipelines, and tunnels. During the past three decades, significant advances have been made regarding the interface shear behavior of sand-structure interfaces by authors such as [1-6]. This research has explored the effect of surface roughness and hardness, particle size, gradation, angularity, and soil state. Interfaces with fine-grained soils have received less attention, with the effects of shear rate on the strength and deformation behavior receiving attention in recent years.

Important work by [7-9] focused on the influence of surface roughness on the interface shear behavior of fine-grained soil. Other studies by [10-13] have highlighted the influence at viscosity effects on the strength behavior on soil-on-soil tests. Studies by [14-16] have shown that the drainage conditions at the interface transition from

[1] Corresponding Author, Department of Civil and Environmental Engineering, University of California Davis, 2001 Ghausi Hall, 1 Shields Ave., Davis, CA USA

drained to partially drained to undrained as the shearing rate is increased, leading to accumulation of excess pore pressures. The shearing rate at which drainage conditions change depends on clay mineralogy, plasticity, coefficient of consolidation, stress level, and stress history [17-19]. The study described herein focuses on aspects of clay interface shear behavior that have received less attention, including the coupled effects of shear rate, stress history, and surface roughness on the strength and deformation behavior at the element- and meso-scales.

2. Materials and methods

2.1. Tested soil and surfaces

All specimens consisted of kaolin clay from Amberger Kaolin Werke (Germany). The kaolin has 52% particles smaller than 2 μm, its liquid limit is 59.8%, its compression and swelling indices are 0.31 and 0.14, respectively, and its coefficient of consolidation for normally-consolidated (NC) specimens is 0.007 cm/s^2. Other properties are included in Table 1. All specimens were prepared by thoroughly mixing dry kaolin with deionized water to a water content equivalent to 1.2 times the liquid limit. As described in [20], the slurry was initially consolidated in large consolidation molds to a stress equivalent to 70% of the final target consolidation stress. Then, the specimens were extruded, trimmed to a cross section area of 100 mm by 64 mm, and speckles were added to one side to enhance its color texture for Particle Image Velocimetry (PIV) analysis. The samples were then transferred to the shear box where they were consolidated to the target stress level.

Table 1. Kaolin clay properties.

Particle Aspect Ratio[a]	28:1
Particle Specific Gravity (g/cm^3)	2.66
Liquid Limit, L_L (%)	59.8
Plastic Limit, P_L (%)	33.9
Plasticity Index (%)	25.9
% of particles by mass smaller than 2 μm[b]	52
Compression Index, C_C	0.31
Swelling Index, C_S	0.14
Coefficient of Consolidation, C_V (cm^2/s)[c]	0.01

[a]Reported by manufacturer, [b]from Hydrometer test, [c]For normally-consolidated specimens

Interface shear tests were performed against two different surfaces: one consisting of a steel plate with epoxied sand, with an average roughness (R_a) of 99.47 μm (referred to as the rough surface), and the second one consisting of a sandblasted steel plate with R_a of 0.94 μm (referred to as the medium rough surface), as described in [20]. Profiles of both surfaces, obtained with a Keyence VR-3100 white light scanner (Japan), are presented in Figures 1a and 1b. As shown, the R_a magnitude for the rough surface is roughly 100 times larger than that for the medium rough surface.

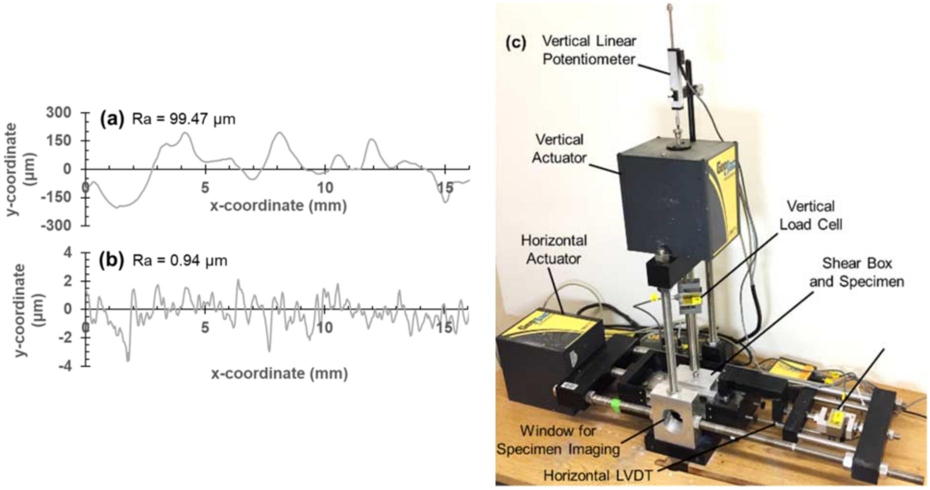

Figure 1. Surface profile of (a) rough and (b) medium rough surfaces (note different y-axis), and (c) interface shear box testing device.

2.2. Interface shear tests

The interface shear testing device consists of a direct shear device adapted with a plate on which the testing surface is mounted, as shown in Figure 1c. The soil specimen is placed on top of the testing surface, and normal load is applied to it by an actuator. A horizontal actuator displaces the testing surface to create relative displacement between the surface and the soil specimen. Load cells and linear potentiometers attached in series with the vertical and horizontal actuators measure the normal and shear loads and displacements. The friction between the box and the surface was measured as 1.5 kPa, which was subtracted from all measured shear stresses. All specimens tested as part of this study were either NC or over-consolidated (OC, OCR = 5). The applied normal stress, σ_n, was either 75 or 150 kPa. The testing shear rate was between 0.006 and 4 mm/min. Further details on the testing procedure are provided in [20].

One of the side walls of the shear box consists of a glass window that allowed for imaging of the specimens throughout testing. Images were taken with an SLR Nikon D3100 camera (14.2 megapixels) with a 35 mm focal length lens. Images were acquired at every 0.05 mm of displacement of the testing surface. The GeoPIV-RG open source software [21,22] was used to perform PIV analyses. All analyses were performed with subset sizes between 45 and 70 pixels and a zero-normalized cross-correlation coefficient threshold of 0.85. The horizontal soil displacements reported correspond to averages obtained from the central third portion of the specimen. Further details regarding PIV analysis procedures are provided in [20].

3. Results and discussion

3.1. Normally-consolidated clay

The results of six tests against the rough surface and five tests against the medium rough surface indicate that the mobilized shear stresses and the associated contractive vertical displacements decreased as the testing shear rate was increased. Figures 2a and 2b show the results of tests against the rough surface while Figures 2c and 2d show the results of tests against the medium rough surface. The tests performed at shear rates of 0.006, 0.02, and 0.06 mm/min mobilized a peak shear stress followed by strain softening, while the tests performed at shear rates of 0.2 mm/sec and faster exhibited a hardening response. The contractive vertical displacements exhibited by specimens sheared at a rate of 1 and 4 mm/min were as small as 0.1 mm, in contrast to the vertical displacements of up to 0.7 mm exhibited by the specimen sheared at 0.02 mm/min against the rough surface.

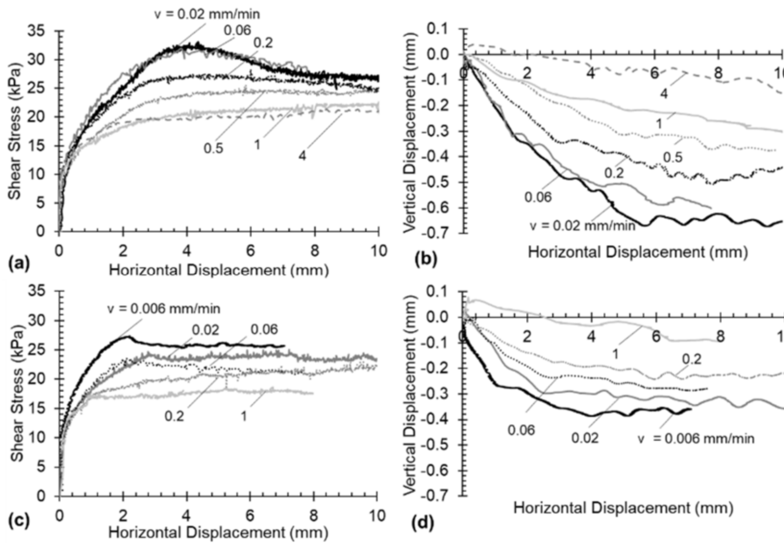

Figure 2. Shear stress – horizontal displacement and vertical displacement – horizontal displacement curves for tests on NC specimens against (a) and (b) rough and (c) and (d) medium rough surfaces (σ_n = 75 kPa).

The mobilized drainage conditions at the interface progressively shifted from drained to undrained as the shear rate was increased, in agreement with results from [14,16]. The change in drainage conditions is highlighted by the decrease in mobilized shear resistances due to generation of excess pore pressures, and by the decrease in induced vertical displacement due to the mobilized near constant volume conditions. Failure envelopes with power law functions were constructed for the interfaces with rough and medium rough surfaces from results of tests at slow shear rates (0.02 mm/min), as shown in Figures 3a and 3b, respectively. Additional tests at the same stress level but at faster shear rates indicate that the stress paths, inferred using the Boukpeti and White [16] framework, converge to the failure envelopes, providing evidence of the accumulation of excess pore pressures.

3.2. Over-consolidated clay

The tests on OC specimens sheared against rough and medium rough surfaces indicate an increase in mobilized shear resistances and a decrease in volumetric changes as the shear rate was increased, as shown in Figures 4a through 4d. Both the shear stress and the volumetric changes indicate a dilative response characterized by strain softening behavior and an increase in specimen volume. The dilative behavior of the specimens led to generation of negative excess pore pressures that result in an increase in the effective stress at the interface, as shown in the inferred stress paths are shown in Figures 3a and 3b.

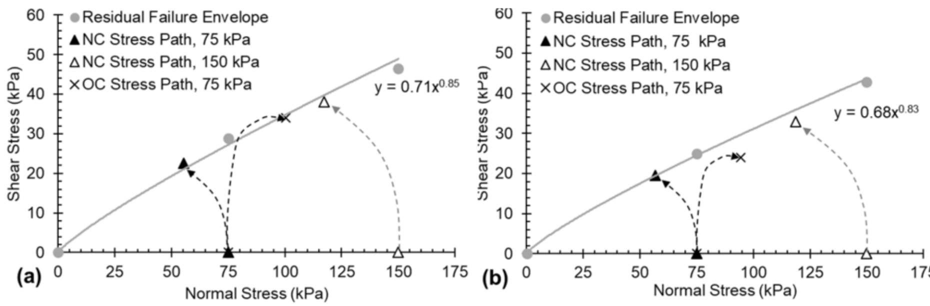

Figure 3. Residual failure envelopes and inferred undrained stress paths for tests on NC and OC specimens against (a) rough and (b) medium rough surfaces.

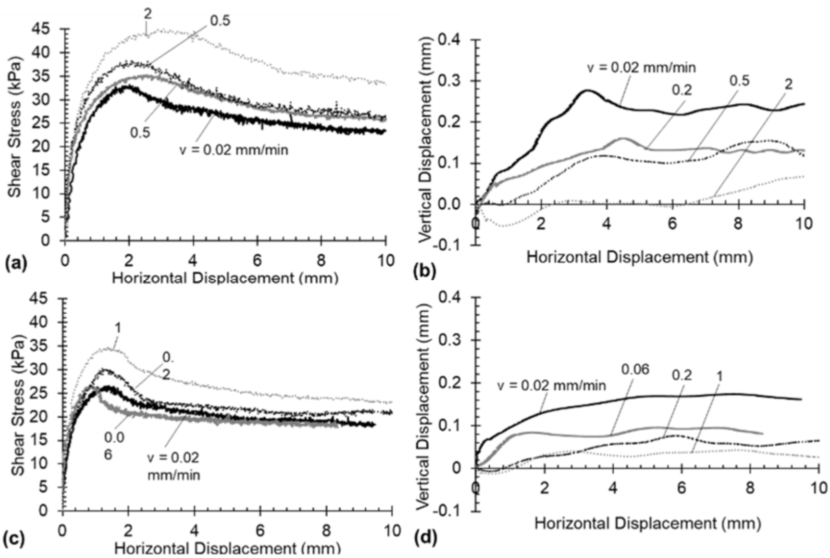

Figure 4. Shear stress – horizontal displacement and vertical displacement – horizontal displacement curves for tests on OC specimens against (a) and (b) rough and (c) and (d) medium rough surfaces (σ_n = 75 kPa).

3.3. Effect of shear rate on interface shear strength

The rate at which the specimens were deformed controlled the drainage conditions and associated accumulation of excess pore pressures. The NC specimens generated positive excess pore pressures that resulted in a decrease in the mobilized peak and residual shear resistances, as shown in Figures 5a and 5b in terms of the stress ratio (τ/σ_n). As shown, a larger interface strength was mobilized by the rough surface at any given shear rate (i.e. shear velocity). The results indicate a coupled effect between surface roughness and shear rate since the rate at which the drainage conditions transitioned from drained to partially drained and from partially drained to undrained are different for tests against the rough and medium rough surfaces. For instance, the conditions transitioned from drained to partially drained at rates faster than 0.06 mm/min for tests against the rough surface, and at rates larger than 0.006 mm/min for tests against the medium rough surface. Similarly, the conditions transitioned to undrained conditions at shear rates faster than 4 mm/min for tests against the rough surface and at rates faster than 1 mm/min for tests against the medium rough surface. The results from tests on OC specimens indicate an increase in strength with shear rate, and a similar coupled effect between shear rate and surface roughness, as shown in Figures 5c and 5d.

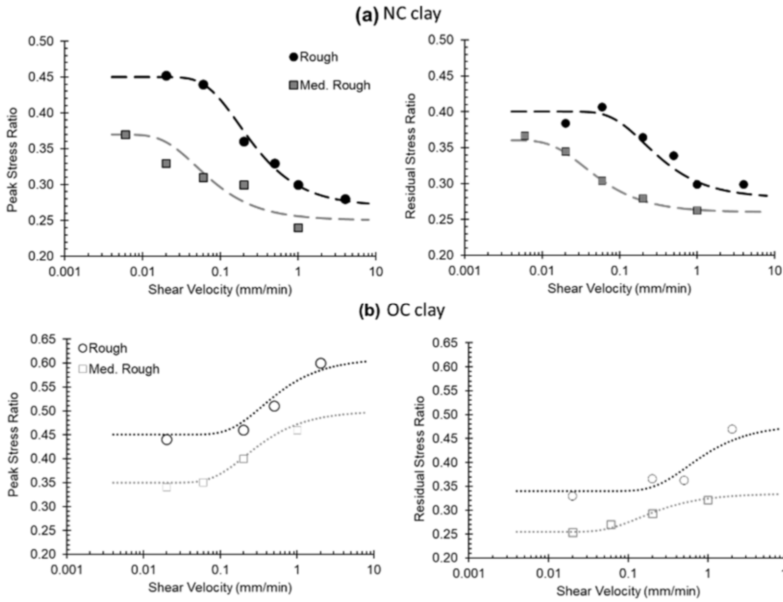

Figure 5. Peak and residual stress ratio as a function of shear velocity for (a) NC and (b) OC specimens.

3.4. Effect of shear rate on meso-scale soil deformations

PIV analysis of the images obtained during tests on NC specimens indicate that shearing against the rough surface led to larger soil horizontal deformations that were developed over a larger zone, as shown in Figures 6a and 6b. While the deformations against the medium rough surface localized in a zone smaller than 1 mm from the interface, the corresponding deformations for the test against the rough surface are not as clearly localized. An increase in shear rate resulted in a significant decrease in soil deformations for tests against both rough and medium rough surfaces. This is shown in the soil deformations in the tests performed at 1.0 mm/min that are significantly smaller than those in the tests at 0.02 mm/min (Figures 6c and 6d). The effect of shearing velocity indicates a transition in failure mode from intense shearing within a well-developed shear zone during slow, drained tests to primarily sliding between the soil specimen and the surface during fast, undrained tests. The internal soil deformation measurements presented herein highlight the more intense soil shearing induced by rougher surfaces as well as the undrained shearing mechanisms present in tests performed shear rates larger than or equal to 1 mm/min. The latter point is due to undrained shearing enforcing near constant volume conditions that limit the soil deformations and result in a sliding interface failure.

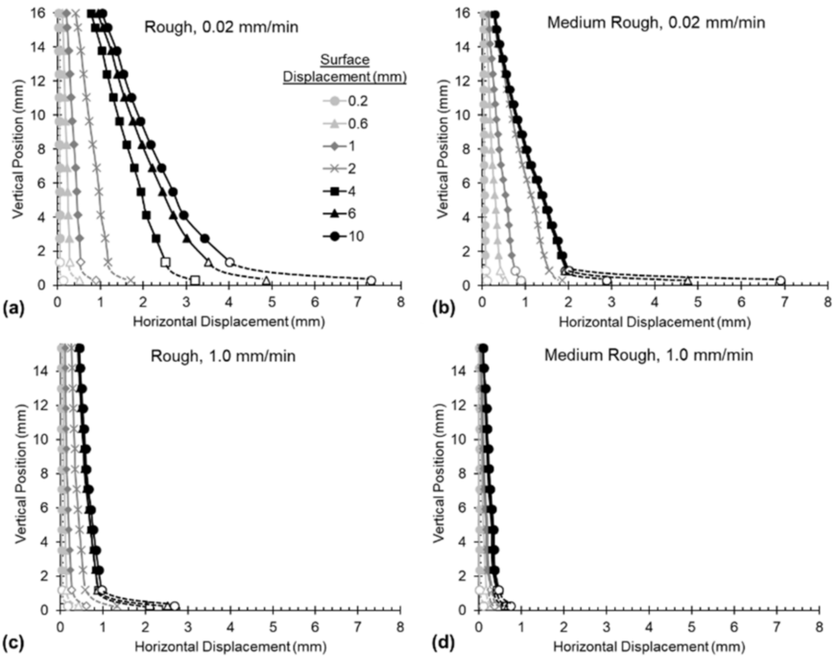

Figure 6. Soil horizontal displacements from tests at 0.02 mm/min against (a) rough and (b) medium rough surfaces, and from tests at 1.0 mm/min against (c) rough and (d) medium rough surfaces.

4. Conclusions

This paper presents the results of shear box interface shear tests performed on normally- and over-consolidated specimens against surfaces of varying roughness and performed at different shear rates. The tests were complemented with PIV analysis to reveal the effect of surface roughness and shear rate on the internal meso-scale soil deformation mechanisms. The laboratory tests indicate that the drainage conditions at the interface transitioned from drained to partially drained to undrained as the shear rate was increased. For NC specimens, the mobilized shear resistances decreased with increasing shear rate due to generation of positive excess pore pressures. On the other hand, the mobilized shear resistance for OC specimens increased as the shear rate was increased due to generation of negative pore pressures. The shear resistance-shear rate relationships provided herein indicate a coupled effect with surface roughness, were shearing against rougher surfaces favored mobilization of drained conditions.

Soil deformations, at the element- and meso-scales, decreased as shear rate was increased. Measurements of soil vertical displacements indicate near constant volume conditions mobilized during tests at a shear rate larger than or equal to 1 mm/min. The NC tests exhibited an overall contractive response while the OC specimens dilated. The horizontal soil displacements obtained from PIV analysis indicate that more intense soil shearing was induced by the rougher surface. In addition, the results highlight the effect of shear rate on the mobilized drainage conditions, where the specimens sheared at fast rates (1 mm/min) underwent considerably smaller deformations than the specimens sheared at slow rates (0.02 mm/min).

Acknowledgements

The first author acknowledges the financial support from the College of Engineering and the Civil and Environmental Engineering Department of the University of California Davis. The second author acknowledges the support by the Cluster of Excellence 80 'The Future Ocean', funded within the framework of the Excellence Initiative by the Deutsche Forschungsgemeinschaft (DFG) on behalf of the German federal and state governments.

References

[1] Uesugi, M., and Kishida, H. Frictional resistance at yield between dry sand and mild steel. *Soils and Foundations*, 26(4) 1986, 139–149.

[2] Dove, J.E. and Frost, J.D. Peak friction behavior of smooth geomembrane-particle interfaces. *Journal of Geotechnical and Geoenviromental Engineering,* 125(7) 1999, 544–555.

[3] DeJong, J. T., Randolph, M. F. and White, D. J. Interface load transfer degradation during cyclic loading: a microscale investigation. *Soils and Foundations*, 43(4) 2003, 81–93.

[4] Dietz, M. S. and Lings, M. L. Post-peak strength of interfaces in a stress-dilatancy framework. *Journal of Geotechnical and Geoenviromental Engineering*, 132(11) 2006, 1474–1484.

[5] DeJong, J.T. and Westgate, Z.J. Role of initial state, material properties, and confinement condition on local and global soil-structure interface behavior. *Journal of Geotechnical and Geoenvironmental Engineering*, 135(11) 2009, 1646-1660.

[6] Martinez, A., and Frost, J.D. The influence of surface roughness form on the strength of sand–structure interfaces. *Géotechnique Letters*, 7(1) 2017, 104–111.

[7] Potyondy, J. G. Skin Friction between Various Soils and Construction Materials. *Géotechnique*, 11 1961, 339–353.

[8] Tsubakihara, Y. and Kishida, H. Frictional behaviour between normally consolidated clay and steel by two direct shear type apparatuses. *Soils and Foundations*, 33(2) 1993, 1–13.

[9] Chen, X., Zhang, J., Xiao, Y. and Li, J. Effect of Roughness on Shear Behavior of Red Clay–concrete Interface in Large-scale Direct Shear Tests. *Canadian Geotechnical Journal*, 52(8) 2015, 1122–1135.

[10] Briaud, J-L. and Garland, E. Loading rate method for pile response in clay. *Journal of Geotechnical Engineering*, 111(3) 1985, 319-335.

[11] Sheahan, T.C., Ladd, C.C. and Germaine, J.T. Rate-dependent undrained shear behavior of saturated clay. *Journal of Geotechnical Engineering*, 122(2) 1996, 99-108.

[12] Sorensen, K. K., Baudet, B. A. and Simpson, B. Influence of structure on the time-dependent behaviour of a stiff sedimentary clay. *Géotechnique*, 57(9) 2007, 783–787.

[13] Brown, M.J. and Hyde, A.F.L. Rate effects from pile shaft resistance measurements. *Canadian Geotechnical Journal*, 45(3) 2008, 425-431.

[14] Lemos, L. J. L. and Vaughan, P. R. Clay - interface shear resistance. *Géotechnique*, 50(1) 2000, 55–64.

[15] Quinn, T.A.C., Robinson, S. and Brown, M.J. High strain rate characterisation of kaolin and its application to rapid load pile testing. *In Proceedings of 9th International Conference on Testing & Design Methods for Deep Foundations* (IS Kanazawa 2012), Kanazawa, Japan, 2012, 311-319.

[16] Boukpeti, N. and White, D. J. Interface shear box tests for assessing axial pipe–soil resistance. *Géotechnique*, 67(1) 2017, 18–30.

[17] Lupini, F., Skinner, A. E. and Vaughan, P. R. The drained residual strength of cohesive soils. *Géotechnique*, 31(2) 1981, 181–213

[18] Steenfelt, J.S. Sliding resistance for foundations on clay till, Predictive soil mechanics. Thomas Telford, London, UK 1992.

[19] Vaughan, P. R., Lemos, L. J. L. J. and Tika-Vassolokos, T. E. Fast shearing of pre-existing shear zones in soil. *Géotechnique*, 46(2) 1996, 197–233.

[20] Martinez, A and Stutz, H.H. Rate effects on the interface shear behaviour of normally and overconsolidated clay. *Accepted for publication in Geotechnique* 2019.

[21] Stanier, S., Blaber J., Take, W. and White D.J. Improved image-based deformation measurement for geotechnical applications. *Canadian Geotechnical Journal*, 53(3) 2015, 727-739.

[22] Stanier, S., Dijkstra, J., Leśniewska, D., Hambleton, J., White, D.J. and Muir Wood, D. Vermiculate artefacts in image analysis of granular materials. *Computers and Geotechnics*, 72 2016, 100–113.